Journal of Engineering Mathematics **38:** 219–232, 2000.

Rheological behavior of a confined bead-spring cube consisting of equal Fraenkel springs

A.I.M. DENNEMAN*, R.J.J. JONGSCHAAP and J. MELLEMA
Twente Institute of Mechanics and J. M. Burgers Centre for Fluid Dynamics Rheology Group, Faculty of Applied Physics, University of Twente P.O. Box 217, 7500 AE Enschede, The Netherlands

Received 29 May 1999; accepted in final form 10 October 1999

Abstract. A general bead-spring model is used to predict linear viscoelastic properties of a non-Hookean bead-spring cube immersed in a Newtonian fluid. This $K \times K \times K$ cube consist of K^3 beads with equal friction coefficients and $3K^2(K-1)$ equal Fraenkel springs with length q. The cube has a topology based upon a simple cubic lattice and it is confined to a container of volume $V_\mathrm{S} = (Kq)^3$. The confined cube is subjected to a small-amplitude oscillatory shear flow with frequency ω, where the directions of the flow velocity and its gradient coincide with two principal directions of the simple cubic bead-spring structure. For this flow field an explicit constitutive equation is obtained with analytical expressions for the relaxation times and their strengths. It is found that the resulting relaxation spectrum belonging to a $K \times K \times K$ Fraenkel cube has the same shape as the one belonging to a 'two-dimensional' $K \times K$ cubic network consisting of equal Hookean springs. On the other hand, the dynamic moduli $G'(\omega)$ and $G''(\omega)$ belonging to a $K \times KK$ Fraenkel cube appear to have the same frequency-dependency as the ones belonging to a 'three-dimensional' $K \times KK$ cube consisting of equal Hookean springs.

Key words: rheology, bead-spring cube, Fraenkel springs, relaxation spectra, dynamic moduli

1. Introduction

To predict the rheological properties of a dilute solution of flexible polymer molecules in a Newtonian fluid several bead-spring models have been developed. The Rouse model [1, 2] constitutes the basis of many of these bead-spring models; only one of these models incorporated the possibility to choose bead-spring structures with an arbitrary topology instead of linear chains (see Sammler and Schrag [3–5]). Recently, we have developed a new bead-spring formalism [6], which provides the mathematical justification for the intuitive results obtained by Sammler and Schrag.

This new bead-spring formalism has already been used to predict the linear viscoelastic properties of a cubic bead-spring structure of arbitrary size immersed in a Newtonian fluid [7]. The topology of this cube was based upon the well-known cubic crystals (simple, body-centered, or face-centered cubic lattice) and it consisted of equal Hookean springs and beads with equal friction coefficients. An explicit constitutive equation was obtained with three sets of relaxation times belonging to the three types of bead-spring cubes (SC, BCC, and FCC). In case of a small-amplitude oscillatory shear flow with frequency ω the obtained dynamic moduli $G'(\omega)$ and $G''(\omega)$ did not show a significant dependency on the specific cubic topol-

* Author to whom all correspondence should be addressed. Present address: Delft University of Technology, Department of Applied Earth Sciences, Section Applied Geophysics & Petrophysics, P.O. Box 5028, 2600 GA, Delft, The Netherlands. Electronic mail: arthur@delphi.tn.tudelft.nl

ogy (in a qualitative sense), although the three relaxation spectra (SC, BCC, and FCC) were significantly different.

The obtained relaxation spectrum belonging to a large Hookean bead-spring cube is quite intriguing: for a sufficiently large cube the discrete relaxation spectrum is changed into a 'continuous' one in which a small number of discontinuities can be observed. These discontinuities are closely related to the so-called Van Hove singularities [8, 9], which are well-known in solid-state physics [10]. In solid-state physics it has already been observed that a periodic ordering of atoms will result in one or more Van Hove singularities and we therefore considered in [8] the following three Hookean systems: (i) a linear chain (K beads, $K-1$ springs), (ii) a 'two-dimensional' $K \times K$ cubic network, or (iii) a 'three-dimensional' $K \times K K$ cube (with a simple cubic topology) immersed in a Newtonian fluid. In case that the size parameter K is sufficiently large, the obtained 'continuous' relaxation spectra belonging to these three Hookean systems (equal springs and beads with equal friction coefficients) show clearly one, two and three discontinuities, respectively, *i.e.*, the number of Van Hove singularities appears to be associated with the dimension of the Hookean structure. Although all these Hookean structures have a topology based upon a crystalline lattice, this does not necessarily imply the same kind of bead ordering in real space. Actually, due to the Hookean character of the springs, a crystal-like ordering of the beads in real space is, in general, by no means present.

In this paper we will consider a bead-spring system which does have a crystal-like bead ordering in real space, *i.e.*, we will consider a cube immersed in a Newtonian fluid in which the Hookean springs are replaced by equal springs of the Fraenkel type [2, 11]. This Fraenkel bead-spring cube (with equal friction coefficients for the beads) has a topology based upon a simple cubic lattice and it is confined to a cubic container in such a way that it cannot rotate freely anymore.

The main difference between a Hookean simple cubic structure and a confined Fraenkel one is the absence and presence, respectively, of the simple cubic ordering of the beads in real space. One of the aims of this paper is to investigate if this difference in bead ordering will result in different linear viscoelastic properties. To that end, we will try to answer the following questions: In what way do the relaxation spectrum and the dynamic moduli $G'(\omega)$ and $G''(\omega)$ belonging to the confined Fraenkel cube differ from the ones belonging to the Hookean cases mentioned before? In case that the Fraenkel cube is sufficiently large, does one obtain a 'continuous' relaxation spectrum? If so, how many Van Hove singularities can be distinguished?

The outline of this paper is as follows. In Section 2 we discuss some general aspects that are independent of the spring characteristics. In Section 3 we start to model the system consisting of a Fraenkel bead-spring cube immersed in a Newtonian fluid, which is confined to a cubic container. In Section 4 we restrict ourselves to a small-amplitude oscillatory shear flow, where the directions of the flow velocity and its gradient coincide with two principal directions of the simple cubic bead-spring structure. For such a flow field the following results are obtained: (i) relaxation spectra for four different sizes of the Fraenkel cube (*i.e.*, 25^3, 50^3, 100^3, and 1000^3 beads), (ii) an exact calculation of the dynamic moduli $G'(\omega)$ and $G''(\omega)$ for a large Fraenkel cube (*i.e.*, 1000^3 beads), and (iii) asymptotic expressions for the dynamic moduli valid for a Fraenkel cube of arbitrary size. We end this paper by giving some concluding remarks in Section 5.

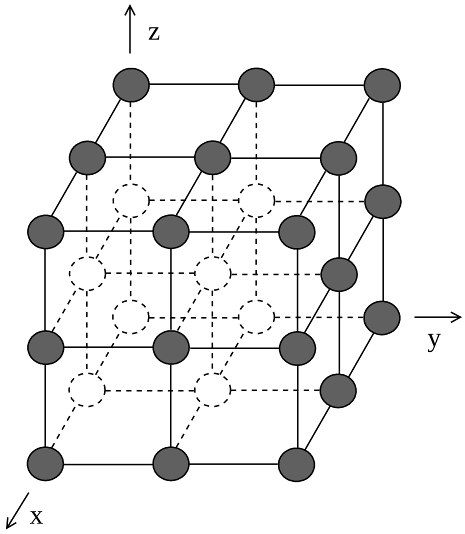

Figure 1. A $3 \times 3 \times 3$ bead-spring cube consisting of 27 beads and 54 springs. The three principal directions of the cubic structure are denoted by x, y, and z.

2. Some general aspects that are independent of spring characteristics

2.1. Some matrices

In this paper we consider a bead-spring structure immersed in a Newtonian fluid with a topology based upon a simple cubic lattice. In Figure 1 a $3\times3\times3$ bead-spring cube is shown, where the directions x, y, and z correspond to the three principal directions of the cubic structure.

In general, a $K\times KK$ bead-spring cube with a topology based upon a simple cubic lattice consists of $N = K^3$ beads and $M = 3K^2(K-1)$ springs and we denote the N bead position vectors and the M connector vectors by the symbols $\mathbf{r}_i$ and $\tilde{\mathbf{r}}_a$, respectively. These two vector sets are interrelated to each other through a topology matrix $\tilde{G}$ as

$$\tilde{\mathbf{r}}_a = \sum_{i=1}^{N} \tilde{G}_{ai}\mathbf{r}_i. \tag{1}$$

The particular values of the matrix elements of $\tilde{G}$ depend upon the chosen directions of the connector vectors and upon the schemes used to number the bead position vectors $\mathbf{r}_i$ and to number the connector vectors $\tilde{\mathbf{r}}_a$. An appropriate way of numbering leads to [7, 8]

$$\tilde{G} = \begin{pmatrix} \tilde{G}^{\mathrm{x}} \\ \tilde{G}^{\mathrm{y}} \\ \tilde{G}^{\mathrm{z}} \end{pmatrix} = \begin{pmatrix} G \otimes \delta_K \otimes \delta_K \\ \delta_K \otimes G \otimes \delta_K \\ \delta_K \otimes \delta_K \otimes G \end{pmatrix}, \tag{2}$$

where the submatrices $\tilde{G}^x$, $\tilde{G}^y$, and $\tilde{G}^z$ are associated with the springs in the x-, y-, and z-direction, respectively.

The symbol $\otimes$ used in Equation (2) denotes the so-called Kronecker product [12, 13], which is defined for an arbitrary $P \times Q$ matrix X and an arbitrary $R \times S$ matrix Y as

$$X \otimes Y \equiv \begin{pmatrix} X_{11}Y & \dots & X_{1Q}Y \\ \vdots & \ddots & \vdots \\ X_{P1}Y & \dots & X_{PQ}Y \end{pmatrix}, \tag{3}$$

so $X \otimes Y$ is a $PR \times QS$ matrix.

The matrix δ_K in Equation (2) is a $K \times K$ identity matrix and the $(K-1) \times K$ matrix G in Equation (2) is defined as

$$G_{ij} = \delta_{i(j-1)} - \delta_{ij} \quad \text{with} \quad \begin{cases} i = 1 \dots (K-1) \\ j = 1 \dots K, \end{cases} \tag{4}$$

in which δ_{ij} is the Kronecker delta ($\delta_{ij} = 1$ if $i = j$, $\delta_{ij} = 0$ if $i \neq j$). It is noted that this matrix G is identical to the topology matrix $\tilde{G}$ belonging to a linear Rouse chain consisting of K beads and $K-1$ springs [2, 8].

The symmetric matrix $A = \tilde{G}^T \tilde{G}$ is a generalization of a matrix used by Rouse [1, 2] and it is given by

$$A = A^x + A^y + A^z, \tag{5}$$

where the symmetric matrices $A^x = \tilde{G}^{x^T} \tilde{G}^x$, $A^y = \tilde{G}^{y^T} \tilde{G}^y$, and $A^z = \tilde{G}^{z^T} \tilde{G}^z$ are given by

$$A^x = G^T G \otimes \delta_K \otimes \delta_K, \tag{6}$$

$$A^y = \delta_K \otimes G^T G \otimes \delta_K, \tag{7}$$

$$A^z = \delta_K \otimes \delta_K \otimes G^T G. \tag{8}$$

These four matrices A, A^x, A^y, and A^z can be diagonalized simultaneously by a transformation matrix Q as follows:

$$(Q^T A^x Q)_{ij} = (\Lambda\Lambda \otimes \delta_K \otimes \delta_K)_{ij} = a_i^x \delta_{ij}, \tag{9}$$

$$(Q^T A^y Q)_{ij} = (\delta_K \otimes \Lambda\Lambda \otimes \delta_K)_{ij} = a_i^y \delta_{ij}, \tag{10}$$

$$(Q^T A^z Q)_{ij} = (\delta_K \otimes \delta_K \otimes \Lambda\Lambda)_{ij} = a_i^z \delta_{ij}, \tag{11}$$

$$(Q^T A Q)_{ij} = (a_i^x + a_i^y + a_i^z)\delta_{ij}, \tag{12}$$

where Q is a $K^3 \times K^3$ orthogonal transformation matrix (*i.e.*, $Q^{-1} = Q^T$) and the diagonal matrix Λ in Equations (9), (10), and (11) is defined as

$$\Lambda_{ij} = 2 \sin\left(\frac{(i-1)\pi}{2K}\right) \delta_{ij} \quad \text{with} \quad \begin{cases} i = 1 \dots K \\ j = 1 \dots K. \end{cases} \tag{13}$$

For example, for $K = 2$ the three sets of eigenvalues are $a^x = (0\,0\,0\,0\,2\,2\,2\,2)$, $a^y = (0\,0\,2\,2\,0\,0\,2\,2)$, and $a^z = (0\,2\,0\,2\,0\,2\,0\,2)$.

The expression for the orthogonal transformation matrix Q is given by

$$Q = (R \otimes R \otimes R) \quad \text{with} \quad R = \begin{pmatrix} \frac{1}{\sqrt{K}} V_K & G^T \Omega \Gamma^{-1} \end{pmatrix}, \tag{14}$$

in which the column vector V_K is a $K \times 1$ vector with all its elements equal to one, the matrix G is defined by Equation (4), and the symmetric matrix Ω and diagonal matrix Γ are defined as

$$\Omega_{ij} = \sqrt{\frac{2}{K}} \sin\left(\frac{ij\pi}{K}\right) \quad \text{with} \quad \begin{cases} i = 1 \ldots (K-1) \\ j = 1 \ldots (K-1), \end{cases} \tag{15}$$

$$\Gamma_{ij} = 2 \sin\left(\frac{i\pi}{2K}\right) \delta_{ij} \quad \text{with} \quad \begin{cases} i = 1 \ldots (K-1) \\ j = 1 \ldots (K-1). \end{cases} \tag{16}$$

We note that the $(K-1) \times (K-1)$ matrix GG^T is diagonalized by the orthogonal transformation matrix Ω defined by Equation (15), while the eigenvalues of GG^T are equal to the squares of the diagonal elements of matrix Γ defined by Equation (16), *i.e.*, $\Omega^T GG^T \Omega = \Gamma\Gamma$ [2]. On the other hand, the $K \times K$ matrix $G^T G$ is diagonalized by the orthogonal transformation matrix R defined in Equation (14), *i.e.*, $R^T G^T G R = \Lambda\Lambda$, where the diagonal matrix Λ is defined in Equation (13).

2.2. Some equations

The configuration of a $K \times KK$ bead-spring cube changes in time according to the equation of motion for the $N = K^3$ bead position vectors $\mathbf{r}_i$ given by [6, 7]

$$\dot{\mathbf{r}}_i = \mathbf{L} \cdot \mathbf{r}_i - \frac{1}{\zeta} \left(kT \frac{\partial \log \psi}{\partial \mathbf{r}_i} + \sum_{a=1}^{M} \tilde{G}_{ai} \tilde{\mathbf{f}}_a \right), \tag{17}$$

where $\tilde{\mathbf{f}}_a$ is the spring force parallel to connector vector $\tilde{\mathbf{r}}_a$, k the Boltzmann constant, T the absolute temperature, $\psi(\mathbf{r}^N, t)$ the distribution function in configuration space of the set of N beads in which t denotes its time-dependency, ζ the friction coefficient belonging to each bead, $\mathbf{L} \cdot \mathbf{r}_i$ the ambient velocity of the solvent at bead i (where $\mathbf{L}$ is the velocity gradient tensor), and $\dot{\mathbf{r}}_i$ the flux velocity of bead i appearing in the equation of continuity for $\psi(\mathbf{r}_{i\,t})$ given by

$$\frac{\partial \psi}{\partial t} = - \sum_{i=1}^{N} \frac{\partial}{\partial \mathbf{r}_i} \cdot (\dot{\mathbf{r}}_i \psi) \, . \tag{18}$$

An expression for the stress tensor $\mathbf{T}$ in terms of microscopic quantities is the so-called ‘Kramers form’ [2, 14], *i.e.*,

$$\mathbf{T} = -p\mathbf{1} + 2\eta_s \mathbf{D} - (N-1)\frac{kT}{V_\mathrm{s}}\mathbf{1} + \frac{1}{V_\mathrm{s}} \sum_{a=1}^{M} \langle \tilde{\mathbf{r}}_a \tilde{\mathbf{f}}_a \rangle, \tag{19}$$

where $\mathbf{1}$ is a unit tensor, p the undetermined pressure, $\mathbf{D} = \frac{1}{2}(\mathbf{L} + \mathbf{L}^T)$ the rate-of-strain tensor, V_s the container volume (in which one bead-spring cube is immersed in a Newtonian fluid of viscosity η_s), and $\langle \cdots \rangle$ denotes an average with respect to the distribution function in configuration space.

3. A confined bead-spring cube consisting of equal Fraenkel springs

In a previous paper [7] we considered a bead-spring cube immersed in a Newtonian fluid, where the spring characteristics were chosen to be Hookean, while the topology of the cube was based upon a simple, body-centered, or face-centered cubic lattice. However, a cubic topology does not necessarily imply a cubic ordering of the beads in real space. Actually, in case of a Hookean cube the actual shape of this bead-spring structure is in general by no means cubic.

To obtain a cubic-like ordering of the beads in real space we consider in this paper a bead-spring cube immersed in a Newtonian fluid, where the Hookean springs are replaced by equal Fraenkel springs. The spring forces $\tilde{\mathbf{f}}_a$ belonging to these Fraenkel springs are defined as [2, 11]

$$\tilde{\mathbf{f}}_a = \kappa \left(1 - \frac{q}{\tilde{r}_a}\right) \tilde{\mathbf{r}}_a, \tag{20}$$

in which κ is the spring constant and q a spring parameter that is strongly related (but not equal) to the equilibrium length of each spring, *i.e.*, the spring force $\tilde{\mathbf{f}}_a$ is zero for $\tilde{r}_a = q$, attractive for $\tilde{r}_a > q$ and repulsive for $\tilde{r}_a < q$. To keep the forthcoming analysis as simple as possible we will only consider the case that the topology of the $K \times K K$ Fraenkel bead-spring cube is based upon the simple cubic lattice and, furthermore, we confine this Fraenkel cube to a cubic container of volume $V_{\mathrm{s}} = Nq^3 = (Kq)^3$.

The beads at the outer surfaces of the Fraenkel cube experience container wall forces. The main effect of these short-range wall forces on the motion of all the beads is to maintain the beads at the simple cubic lattice points in real space. To keep the bead motions largely limited to local excursions centered on these lattice points, the spring constant κ is chosen to be sufficiently large. In the forthcoming modeling we will not include the explicit influence of the wall forces in the equation of motion given by Equation (17), *i.e.*, only an implicit effect of the wall forces is taken into account: the simple cubic ordering of the beads in real space. We note that the neglecting of explicit effects of the wall forces is only appropriate for large bead-spring cubes (*i.e.*, the size parameter K should be sufficiently large).

In consequence of this simple cubic ordering of the beads in real space, the motion of the bead position vectors $\mathbf{r}_i$ will take place around the constant vectors $\mathbf{s}_i$, which denote the lattice point positions of the simple cubic lattice. In the same way, the motion of the connector vectors $\tilde{\mathbf{r}}_a$ will take place around the constant vectors $\mathbf{q}_a$. The vectors $\mathbf{q}_a$ are equal to $q\mathbf{e}_x$, $q\mathbf{e}_y$, and $q\mathbf{e}_z$ for springs in the x-, y-, and z-direction, respectively, where the vectors $\mathbf{e}_x$, $\mathbf{e}_y$, and $\mathbf{e}_z$ form a fixed orthonormal basis in space.

In case of a sufficiently large spring constant κ the deviation $\tilde{\mathbf{d}}_a = \tilde{\mathbf{r}}_a - \mathbf{q}_a$ will be small so that Equation (20) may be approximated by its first order Taylor-expansion, *i.e.*,

$$\tilde{\mathbf{f}}_a = \kappa \mathbf{P}_a \cdot \tilde{\mathbf{d}}_a \quad \text{with} \quad \mathbf{P}_a = \frac{\mathbf{q}_a \mathbf{q}_a}{q^2}, \tag{21}$$

where the projection tensor $\mathbf{P}_a$ is equal to $\mathbf{e}_{\mathrm{x}}\mathbf{e}_{\mathrm{x}}$, $\mathbf{e}_{\mathrm{y}}\mathbf{e}_{\mathrm{y}}$, and $\mathbf{e}_{\mathrm{z}}\mathbf{e}_{\mathrm{z}}$ for springs in the x-, y-, and z-direction, respectively. By substituting Equation (21) in Equation (17) and by using a transformation similar to Equation (1) (*i.e.*, $\tilde{\mathbf{d}}_a = \sum \tilde{G}_{ai}\, \mathbf{d}_i$ with $\mathbf{d}_i = \mathbf{r}_i - \mathbf{s}_i$), we obtain the equation of motion for $\mathbf{d}_i$ given by

$$\dot{\mathbf{d}}_i = \mathbf{L} \cdot \mathbf{d}_i + \mathbf{L} \cdot \mathbf{s}_i - \frac{1}{\zeta} \left(kT \frac{\partial \log \psi'}{\partial \mathbf{d}_i} + \kappa \sum_{a=1}^{M} \sum_{b=1}^{N} \tilde{G}_{ai} \tilde{G}_{ab}\, \mathbf{P}_a \cdot \mathbf{d}_b \right), \tag{22}$$

where ψ' is defined as $\psi'(\mathbf{d}^N, t) \equiv \psi(\mathbf{r}^N, t)$.

The relation $V_s = Nq^3$ and the expression for the Fraenkel spring given by Equation (20) are substituted in the expression for the stress tensor $\mathbf{T}$ given by Equation (19), which leads to

$$\mathbf{T} = -p\mathbf{1} + 2\eta_s\mathbf{D} - \frac{(N-1)kT}{Nq^3}\mathbf{1} + \mathbf{T}', \tag{23}$$

where stress $\mathbf{T}'$ is the second order Taylor expansion of the last term on the right hand side of Equation (19), *i.e.*, for small deviations $\tilde{\mathbf{d}}_a = \tilde{\mathbf{r}}_a - \mathbf{q}_a$ this term is given by

$$\mathbf{T}' = \frac{\kappa}{Nq^3}\sum_{a=1}^{M}\left(\langle \mathbf{P}_a \cdot \tilde{\mathbf{d}}_a\tilde{\mathbf{d}}_a + \tilde{\mathbf{d}}_a\mathbf{P}_a \cdot \tilde{\mathbf{d}}_a\rangle + \mathbf{P}_a\langle \mathbf{q}_a \cdot \tilde{\mathbf{d}}_a + \tfrac{1}{2}\tilde{\mathbf{d}}_a \cdot (\mathbf{1} - 3\mathbf{P}_a) \cdot \tilde{\mathbf{d}}_a\rangle\right). \tag{24}$$

4. Small-amplitude oscillatory shear flow

4.1. Constitutive equation

We now restrict ourselves to the case of a small-amplitude oscillatory shear flow with angular frequency ω, where the direction of the flow velocity is in the $\mathbf{e}_x$-direction and its gradient in the $\mathbf{e}_y$-direction, *i.e.*, these two directions coincide with two principal directions of the bead-spring cube (denoted by x and y in Figure 1). For the velocity gradient tensor $\mathbf{L}$ this means that $L_{xy} = \mathrm{i}\omega\gamma_\circ \exp(\mathrm{i}\omega t)$ with amplitude $\gamma_\circ \ll 1$, while the other elements of $\mathbf{L}$ are zero. For such a flow field only the xy-component of the stress tensor $\mathbf{T}$ and the x- and y-coordinates of the deviations $\mathbf{d}_i$ and $\tilde{\mathbf{d}}_a$ are of particular interest.

As mentioned in Section 3 the projection tensor $\mathbf{P}_a$ is equal to $\mathbf{e}_x\mathbf{e}_x$, $\mathbf{e}_y\mathbf{e}_y$, and $\mathbf{e}_z\mathbf{e}_z$ for springs in the x-, y-, and z-direction, respectively. By combining these projection tensors with Equations (22), (23), and (24) we obtain

$$\dot{d}_{i,x} = L_{xy}d_{i,y} + L_{xy}s_{i,y} - \frac{1}{\zeta}\left(kT\frac{\partial \log \psi'}{\partial d_{i,x}} + \kappa\sum_{b=1}^{N}A^x_{ib}d_{b,x}\right), \tag{25}$$

$$\dot{d}_{i,y} = -\frac{1}{\zeta}\left(kT\frac{\partial \log \psi'}{\partial d_{i,y}} + \kappa\sum_{b=1}^{N}A^y_{ib}d_{b,y}\right), \tag{26}$$

$$T_{xy} = L_{xy}\eta_s + \frac{\kappa}{Nq^3}\sum_{i=1}^{N}\sum_{j=1}^{N}\left(A^x_{ij} + A^y_{ij}\right)\langle d_{i,x}d_{j,y}\rangle, \tag{27}$$

where the definitions of matrices A^x and A^y are given by Equations (6) and (7), respectively.

The set of vectors $\mathbf{d}_i$ is transformed into a set of normal coordinate vectors $\boldsymbol{\xi}_i$ by a transformation of the type

$$\mathbf{d}_i = \sum_{j=1}^{N}Q_{ij}\boldsymbol{\xi}_j, \qquad \frac{\partial}{\partial \mathbf{d}_i} = \sum_{j=1}^{N}Q_{ij}\frac{\partial}{\partial \boldsymbol{\xi}_j}, \tag{28}$$

where the orthogonal transformation matrix Q is defined by Equation (14). By using Equations (9), (10), and (28), we transform Equations (25) and (26) into equations of motion in the $\boldsymbol{\xi}$-representation, *i.e.*,

$$\dot{\xi}_{i,x} = L_{xy}\xi_{i,y} + L_{xy}\sum_{j=1}^{N}Q_{ji}s_{j,y} - \frac{1}{\zeta}\left(kT\frac{\partial \log \bar{\psi}'}{\partial \xi_{i,x}} + \kappa a^x_i\xi_{i,x}\right), \tag{29}$$

$$\dot{\xi}_{i,y} = -\frac{1}{\zeta}\left(kT\frac{\partial \log \bar{\psi}\,'}{\partial \xi_{i,y}} + \kappa a_i^y \xi_{i,y}\right), \tag{30}$$

where $\bar{\psi}\,'$ is defined as $\bar{\psi}\,'(\boldsymbol{\xi}^N, t) \equiv \psi\,'(\mathbf{d}^N, t) \equiv \psi(\mathbf{r}^N, t)$ and the sets of eigenvalues a_i^{x} and a_i^{y} are defined by Equations (9) and (10), respectively. In the same way we transform the xy-component of the stress tensor $\mathbf{T}$ given by Equation (27) into the $\boldsymbol{\xi}$-representation, *i.e.*,

$$T_{xy} = L_{xy}\eta_s + \sum_{i=1}^{N} T_{i,xy}^{\mathrm{P}} \quad \text{with} \quad T_{i,xy}^{P} = \frac{\kappa}{Nq^3}\left(a_i^x + a_i^{\mathrm{y}}\right)\langle \xi_{i,x}\xi_{i,y}\rangle, \tag{31}$$

where $\langle \xi_{i,x}\xi_{i,y}\rangle = 0$ for the modes with $a_i^y = 0$. Consequently, the stress $T_{i,xy}^{\mathrm{P}}$ is zero for each normal mode with $a_i^y = 0$ and we only have to consider the modes with $a_i^y \neq 0$.

By transforming the equation of continuity for $\psi(\mathbf{r}^N, t)$ given by Equation (18) into an equation of continuity for $\bar{\psi}\,'(\boldsymbol{\xi}^N, t)$, by multiplying both sides of the resulting equation by $\xi_{i,x}\xi_{i,y}$, and by integrating it over the entire $\boldsymbol{\xi}$-space, we obtain for the modes with $a_i^y \neq 0$:

$$\frac{\mathrm{d}}{\mathrm{d}t}\langle \xi_{i,x}\xi_{i,y}\rangle = \langle \dot{\xi}_{i,x}\xi_{i,y}\rangle + \langle \xi_{i,x}\dot{\xi}_{i,y}\rangle = -\frac{\kappa}{\zeta}\left(a_i^x + a_i^y\right)\langle \xi_{i,x}\xi_{i,y}\rangle + \frac{kT}{\kappa a_i^y}L_{xy}, \tag{32}$$

where we have used the relations

$$\langle \xi_{i,y}\rangle = 0, \qquad \langle \xi_{i,y}^2\rangle = \frac{kT}{\kappa a_i^y}, \qquad \left\langle \boldsymbol{\xi}_i \frac{\partial \log \bar{\psi}\,'}{\partial \boldsymbol{\xi}_i}\right\rangle = -\mathbf{1}. \tag{33}$$

By combining Equations (31) and (32) we obtain a constitutive equation for $T_{i,xy}^P$, *i.e.*,

$$\text{for } a_i^y = 0 \qquad T_{i,xy}^P = 0, \tag{34}$$

$$\text{for } a_i^y \neq 0 \qquad \frac{\mathrm{d}T_{i,xy}^P}{\mathrm{d}t} + \frac{1}{\lambda_i}T_{i,xy}^P = \mu_i \frac{kT}{Nq^3}L_{xy}, \tag{35}$$

with the relaxation times λ_i and the relaxation strengths μ_i given by

$$\lambda_i = \frac{\zeta}{\kappa\left(a_i^x + a_i^y\right)}, \qquad \mu_i = 1 + \frac{a_i^x}{a_i^y}. \tag{36}$$

4.2. Relaxation spectrum

By combining Equations (9), (10), (13), and (36), we obtain expressions for the $K^2(K-1)$ relaxation times λ_i and their strengths μ_i which are given by

$$\lambda_i \equiv \lambda_{klm} = \frac{\zeta}{4\kappa\left[\sin^2\left(\dfrac{k\pi}{2K}\right) + \sin^2\left(\dfrac{l\pi}{2K}\right)\right]}, \tag{37}$$

$$\mu_i \equiv \mu_{klm} = 1 + \frac{\sin^2\left(\dfrac{k\pi}{2K}\right)}{\sin^2\left(\dfrac{l\pi}{2K}\right)} \tag{38}$$

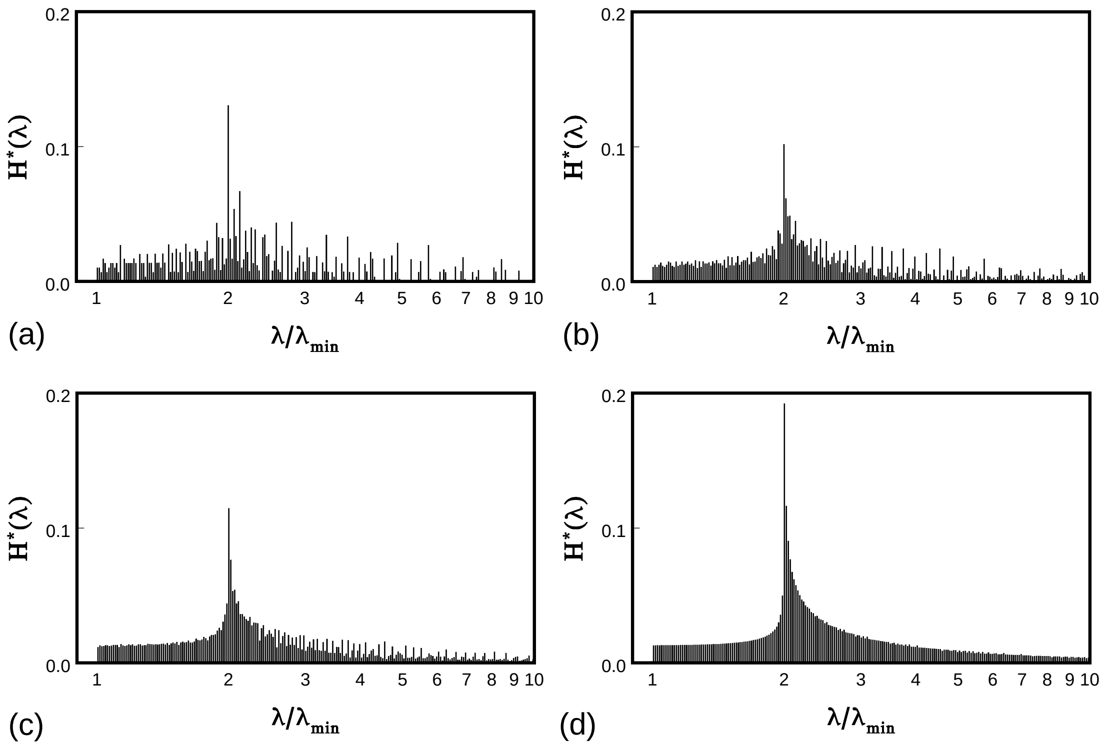

Figure 2. The reduced relaxation spectrum $H^*(\lambda)$ for a confined $K \times KK$ Fraenkel bead-spring cube immersed in a Newtonian fluid: (a) $K = 25$, (b) $K = 50$, (c) $K = 100$, and (d) $K = 1000$.

with $i = K(K-1)k + K(l-1) + m$, $k = 0 \ldots (K-1)$, $l = 1 \ldots (K-1)$ and $m = 1 \ldots K$. The relaxation times λ_i given by Equation (37) are distributed between minimum and maximum values given by

$$\lambda_{\min} = \frac{\zeta}{8\kappa}, \qquad \lambda_{\max} = \frac{8K^2\lambda_{\min}}{\pi^2} = \frac{\zeta K^2}{\pi^2\kappa}. \tag{39}$$

At this moment it is convenient to introduce a relaxation spectrum $H(\lambda,\ \Delta\log_{10}\lambda)$ that represents a weighted distribution of relaxation times, *i.e.*, $H(\lambda,\ \Delta\log_{10}\lambda)$ is defined as the weighted number of relaxation times λ_i satisfying $\log_{10}\lambda - \Delta\log_{10}\lambda < \log_{10}\lambda_i \leq \log_{10}\lambda + \Delta\log_{10}\lambda$, where the weights belonging to these relaxation times λ_i are equal to their strengths μ_i. For a confined $K \times KK$ Fraenkel bead-spring cube immersed in a Newtonian fluid this spectrum $H(\lambda,\ \Delta\log_{10}\lambda)$ can be calculated by using the expression for the $K^2(K-1)$ relaxation times λ_i and their weights μ_i given by Equations (37) and (38), respectively. In Figure 2 we depict the reduced relaxation spectrum $H^*(\lambda) = H(\lambda,\ 0{\cdot}0022)/K^2(K-1)$ as a function of the reduced time $\lambda/\lambda_{\min}$ for four different sizes of the $K \times KK$ Fraenkel bead-spring cube, *i.e.*, parameter K is equal to 25, 50, 100, and 1000, respectively.

One observes in Figure 2 that the reduced relaxation spectrum $H^*(\lambda)$ converges gradually toward a 'continuous' spectrum if K increases. In Figure 2d one observes that for a $1000 \times 1000 \times 1000$ Fraenkel cube the relaxation spectrum $H(\lambda,\ 0{\cdot}0022)$ represents a continuous function for the regions $\lambda_{\min} < \lambda < 2\lambda_{\min}$ and $2\lambda_{\min} < \lambda \leq 10\lambda_{\min}$ with two Van Hove singularities at the times $\lambda = \lambda_{\min}$ and $\lambda = 2\lambda_{\min}$. This 'continuous' spectrum belonging to a large 'three-dimensional' Fraenkel cube has the same shape as the one belonging to a large 'two-dimensional' $K \times K$ cubic network consisting of equal Hookean springs [8].

At first sight, this result might be somewhat surprising, but there is good explanation for it. To obtain this result we have used in our bead-spring model the first order Taylor-expansion of the Fraenkel force $\tilde{\mathbf{f}}_a$ defined by Equation (20). The linearized Fraenkel force $\tilde{\mathbf{f}}_a$ given by Equation (21) is, however, always in the direction of the constant vector $\mathbf{q}_a$, so if one considers a 'two-dimensional' $K \times K$ substructure of the $K \times KK$ Fraenkel cube (consisting of $K(K-1)$ springs with $\mathbf{q}_a = q\mathbf{e}_x$ and $K(K-1)$ springs with $\mathbf{q}_a = q\mathbf{e}_y$), then the z-components of the $2K(K-1)$ spring forces $\tilde{\mathbf{f}}_a$ of this particular $K \times K$ substructure are always equal to zero. One might therefore say that the $K \times KK$ Fraenkel cube consists of K 'two-dimensional' $K \times K$ substructures (with only springs in the x-direction and y-direction), which are interconnected by $K^2(K-1)$ springs in the z-direction (note that the $K \times KK$ Fraenkel cube is subjected to a small-amplitude oscillatory shear flow with the flow velocity in the $\mathbf{e}_x$-direction and its gradient in the $\mathbf{e}_y$-direction).

Consequently, it is not really surprising that the expression for the relaxation times λ_i given by Equation (37) is equal to the expression for λ_i belonging to a 'two-dimensional' $K \times K$ cubic network consisting of equal Hookean springs [8]. Note that the relation $\lambda_{kl1} = \ldots = \lambda_{klm} = \ldots = \lambda_{klK}$ (and, in the same way, $\mu_{kl1} = \ldots = \mu_{klm} = \ldots = \mu_{klK}$) reflects our conception that the $K \times KK$ cube consists of K 'two-dimensional' substructures with only springs in the x- and y-direction. On the other hand, the Fraenkel character of the springs in the $K \times KK$ cube and the presence of springs in the z-direction (which interconnect K 'two-dimensional' substructures) are reflected by the expression for the relaxation strengths μ_i given by Equation (38), which is clearly different from the relation $\mu_i = 1$ valid for the 'two-dimensional' Hookean case [8].

This difference in the Hookean and Fraenkel expressions for the relaxation strengths μ_i leads to a different large K dependency of the reduced relaxation spectrum $H^*(\lambda)$. For the 'two-dimensional' Hookean case it is observed that the spectrum $H^*(\lambda)$ for a sufficiently large $K \times K$ cubic network does not change anymore if one increases the size parameter K [8]. For the $K \times KK$ Fraenkel cube one observes that the large K dependency of $H^*(\lambda)$ is different for the two regions of small and large times λ. In the region of small times (*i.e.*, $\lambda < 2\lambda_{\min}$) there is no difference between the spectrum $H^*(\lambda)$ for $K = 1000$ and the one for a value of K larger than 1000. On the other hand, in the region of large times (*i.e.*, $\lambda \geq 2\lambda_{\min}$) the spectrum $H^*(\lambda)$ for a $K \times KK$ cube with $K \geq 1000$ appears to be smaller than the one belonging to a larger cube, *i.e.*, for large K the maximum value of $H^*(\lambda)$ at $\lambda = 2\lambda_{\min}$ can be approximated by $0{\cdot}0335\log(K) - 0{\cdot}0394$, while similar approximations for $H^*(\lambda)$ are valid for times $\lambda > 2\lambda_{\min}$.

4.3. Dynamic moduli

In Section 4.1 we obtained a constitutive equation for the stress $T^P_{i,xy}$ [see Equations (34) and (35)], which belongs to a confined Fraenkel bead-spring cube immersed in a Newtonian fluid. To obtain this constitutive equation for $T^P_{i,xy}$ we have restricted ourselves to a small-amplitude oscillatory shear flow with frequency ω, where the directions of the flow velocity and its gradient coincide with two principal directions of the simple cubic bead-spring structure.

This constitutive equation for $T^P_{i,xy}$ can be used to determine the dynamical response of the stress T_{xy} given by Equation (31) on the applied flow velocity gradient $L_{xy} = i\omega\gamma_\circ \exp(i\omega t)$, where the elastic and viscous stress response are characterized by the storage modulus $G'(\omega)$

and the loss modulus $G''(\omega)$, respectively. It can be shown (see, *e.g.*., Bird *et al.* [2]) that the constitutive equation for $T^P_{i,xy}$ given by Equations (34) and (35) leads to expressions for the dynamic moduli $G'(\omega)$ and $G''(\omega)$ given by

$$G'(\omega) = \frac{kT}{(Kq)^3} \sum_{i=1}^{K^2(K-1)} \mu_i \frac{(\omega\lambda_i)^2}{1+(\omega\lambda_i)^2}, \tag{40}$$

$$G''(\omega) = \eta_s\omega + \frac{kT}{(Kq)^3} \sum_{i=1}^{K^2(K-1)} \mu_i \frac{\omega\lambda_i}{1+(\omega\lambda_i)^2}, \tag{41}$$

where the relaxation times λ_i and their strengths μ_i are given by Equations (37) and (38), respectively.

Numerical calculations of the dynamic moduli $G'(\omega)$ and $G''(\omega)$ for different sizes of the $K\times KK$ Fraenkel cube will indicate that three different frequency regions can be distinguished, *i.e.*, a low, an intermediate, and a high-frequency region. For each region we obtained asymptotic expressions for the moduli $G'(\omega)$ and $G''(\omega)$ (see Denneman *et al.* [7] and Van der Vorst *et al.* [15] for the method to obtain these asymptotes). The two boundaries of these three frequency regions depend upon the values of the minimum and maximum relaxation times $\lambda_{\min}$ and $\lambda_{\max}$ (see Equation (39) for their definitions).

The asymptotic expressions for the storage modulus $G'(\omega)$ are

$$\omega\lambda_{\min} \ll \omega\lambda_{\max} \ll 1: \quad G'(\omega) = \frac{kT}{q^3}\frac{8(K^4-1)}{5K^2}(\omega\lambda_{\min})^2, \tag{42}$$

$$\omega\lambda_{\min} \ll 1 \ll \omega\lambda_{\max}: \quad G'(\omega) \approx \frac{kT}{q^3}\frac{4(K^2-1)}{3K}(\omega\lambda_{\min})^{3/2}, \tag{43}$$

$$1 \ll \omega\lambda_{\min} \ll \omega\lambda_{\max}: \quad G'(\omega) = \frac{kT}{q^3}\frac{(K-1)(K^2+3K-1)}{3K^2} \tag{44}$$

and the asymptotic expressions for the loss modulus $G''(\omega)$ are

$$\omega\lambda_{\min} \ll \omega\lambda_{\max} \ll 1: \quad G''(\omega) - \eta_s\omega = \frac{kT}{q^3}\frac{4(K^2-1)}{3K}(\omega\lambda_{\min}), \tag{45}$$

$$\omega\lambda_{\min} \ll 1 \ll \omega\lambda_{\max}: \quad G''(\omega) - \eta_s\omega \approx \frac{kT}{q^3}\frac{4(K^2-1)}{3K}(\omega\lambda_{\min}), \tag{46}$$

$$1 \ll \omega\lambda_{\min} \ll \omega\lambda_{\max}: \quad G''(\omega) - \eta_s\omega = \frac{kT}{q^3}\frac{(K-1)(3K^2+17K-16)}{24K^2\,(\omega\lambda_{\min})}. \tag{47}$$

Note that Equations (45) and (46) are identical, *i.e.*, the frequency-dependency of the loss modulus $G''(\omega)$ is in the low frequency region and in the intermediate frequency region the same. Furthermore, by combining Equations (43) and (46) we obtain for the intermediate frequency region $\omega\lambda_{\min} \ll 1 \ll \omega\lambda_{\max}$ an expression which is independent of the size of the $K\times KK$ Fraenkel cube, *i.e.*,

$$\frac{G'(\omega)}{G''(\omega) - \eta_s\omega} \approx (\omega\lambda_{\min})^{1/2}. \tag{48}$$

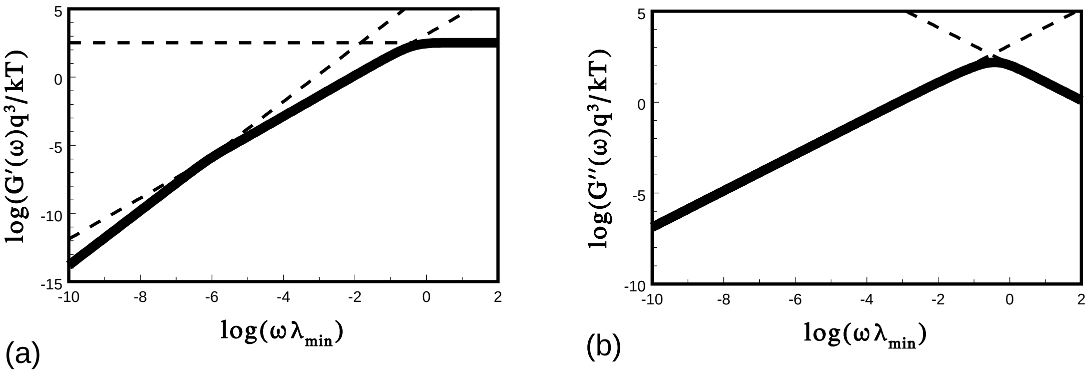

Figure 3. The storage modulus $G'(\omega)$ and the loss modulus $G''(\omega)$ belonging to a confined $1000 \times 1000 \times 1000$ Fraenkel cube immersed in a Newtonian fluid with viscosity $\eta_s = 0$: (a) the reduced storage modulus $\log_{10}(G'(\omega)q^3/kT)$ as a function of reduced frequency $\log_{10}(\omega\lambda_{\min})$ (the dashed lines are the asymptotic expressions given by Equations (42), (43), and (44) and the thick line is its exact calculation) and (b) the reduced loss modulus $\log_{10}(G''(\omega)q^3/kT)$ as a function of reduced frequency $\log_{10}(\omega\lambda_{\min})$ (the dashed lines are asymptotic expressions given by Equations (45), (46), and (47) and the thick line is its exact calculation).

As an example we consider a $1000 \times 1000 \times 1000$ simple cubic bead-spring structure, which consists of equal Fraenkel springs and is immersed in a Newtonian fluid with viscosity $\eta_s = 0$. This Fraenkel cube is confined to a cubic container of volume $V_s = (1000q)^3$, where q is the spring parameter as given in Equation (20). In Figure 3a the three asymptotic expressions given by Equations (42), (43), and (44) are compared with the exact calculation of the expression for $G'(\omega)$ given by Equation (40), and in Figure 3b the three asymptotic expressions given by Equations (45), (46), and (47) are compared with the exact calculation of the expression for $G''(\omega)$ given by Equation (41). In both figures the two boundaries of the three different frequency regions are given by $\log_{10}(\omega\lambda_{\min}) = 0$ and $\log_{10}(\omega\lambda_{\min}) = -5{\cdot}9$ (*i.e.*, $\log_{10}(\omega\lambda_{\max}) = 0$), respectively, and we observe that the asymptotic expressions for the three different frequency regions do approximate the exact calculations very well.

The dynamic moduli $G'(\omega)$ and $G''(\omega)$ belonging to a $K \times KK$ Fraenkel bead-spring cube appears to be similar to the ones belonging to a $K \times KK$ cube consisting of equal Hookean springs [8]. That is, the frequency-dependency of the dynamic moduli (the slopes in Figure 3) is for the ‘three-dimensional’ Fraenkel and Hookean cube exactly the same.

5. Concluding remarks

In this paper we have obtained the relaxation spectrum $H(\lambda, \Delta \log_{10} \lambda)$ and the dynamic moduli $G'(\omega)$ and $G''(\omega)$ belonging to a confined Fraenkel cube immersed in a Newtonian fluid. To obtain these results we have restricted ourselves to a small-amplitude oscillatory shear flow with frequency ω, where the directions of the flow velocity and its gradient coincide with two principal directions of the bead-spring cube.

The obtained relaxation spectrum $H(\lambda, \Delta \log_{10} \lambda)$ belonging to a large $K \times KK$ Fraenkel cube appears to have the same shape as the one belonging to a large ‘two-dimensional’ $K \times K$ cubic network consisting of equal Hookean springs (including the two Van Hove singularities). Actually, the relaxation times λ_i belonging to the ‘three-dimensional’ Fraenkel case and the ‘two-dimensional’ Hookean case appear to be the same, but their strengths μ_i differ. Due to this difference in relaxation strengths the dynamic moduli $G'(\omega)$ and $G''(\omega)$

belonging to the Fraenkel bead-spring cube are not identical to the ones belonging to a 'two-dimensional' Hookean cubic network. Instead, the Fraenkel moduli have exactly the same frequency-dependency as the ones belonging to a 'three-dimensional' Hookean bead-spring cube.

The substitution of $q = 0$ in the expression for the Fraenkel spring force given by Equation (20) leads to a Hookean spring force, so one would expect that the rheological behavior of a confined Fraenkel cube with $q \to 0$ is identical to the rheological behavior of a Hookean cube. Surprisingly, the results obtained in this paper do not fulfill this expectation. Why?

To answer this question it is noted that in the modeling of a $K \times K K$ Fraenkel cube confined in a container of volume $V_s = (Kq)^3$ we have assumed a simple cubic ordering of the beads in real space (in contrast with the Hookean case where this ordering is by no means present). However, in the limit $q \to 0$ this assumption is not valid anymore: (i) the limit $q \to 0$ leads to a non-physical size of the container (*i.e.*, $V_s = (Kq)^3 \to 0$) and (ii) for a decreasing q the influence of the Brownian bead motion in destroying the simple cubic ordering in real space is increased (resulting in a non-ordered system in the limit $q \to 0$). The analysis presented in this paper is therefore only valid in case of a sufficiently large spring parameter q.

Another interesting limit is the 'stiffened' Fraenkel spring limit $\kappa \to \infty$. This limit is not called the rigid rod limit, because there exists a fundamental difference between a stiffened Fraenkel spring and a rigid rod. This difference is associated with some fundamental problems related to the freezing out of a degree of freedom (see, *e.g.*., Gottlieb and Bird [16], Van Kampen [17], and pp. 46–47 in Bird *et al.* [2]). In the stiffened Fraenkel spring limit we obtain $\lambda_{\min} \to 0$ and $\lambda_{\max} \to 0$, which results in dynamic moduli $G'(\omega) \to 0$ and $G''(\omega) \to \eta_s\omega$. This result is in consequence of the confinement of the $K \times K K$ Fraenkel cube to a cubic container of volume $V_s = (Kq)^3$, whereby the orientability of the cube is limited such that it cannot rotate freely anymore.

Although bead-spring models are normally used to model polymer systems, we finally note that we have recently used a model based upon Fraenkel bead-spring cubes to describe successfully the rheological behavior of a colloidal crystal [18]. However, the model based upon Fraenkel cubes presented in the paper on colloidal crystals is not a trivial extension of the model presented in this paper (and *vice versa*).

Acknowledgements

The work described in this paper is part of the research program of the Foundation for Fundamental Research on Matter (FOM), which is supported financially by the Netherlands Organization for Scientific Research (NWO).

References

1. P. E. Rouse, Jr., A theory of the linear viscoelastic properties of dilute solutions of coiling polymers. *J. Chem. Phys.* 21 (1953) 1272–1280.
2. R. B. Bird, C. F. Curtiss, R. C. Armstrong, and O. Hassager, *Dynamics of Polymeric Liquids: Kinetic Theory (vol. 2).* New York: Wiley-Interscience (2nd ed., 1987) 437 pp.
3. R. L. Sammler and J. L. Schrag, *Bead-spring model predictions of solution dynamics for flexible homopolymers incorporating long-chain branches and/or rings. (Tech. Rep. 113).* Wisconsin-Madison: Rheology Research Center (1987) 57 pp.
4. R. L. Sammler and J. L. Schrag, Bead-spring model predictions of solution dynamics for flexible homopolymers incorporating long-chain branches and/or rings. *Macromolecules* 21 (1988) 1132–1140.

5. R. L. Sammler and J. L. Schrag, Predictions of the ability of solution dynamics experiments to characterize long-chain structure in flexible homopolymers. *Macromolecules* 21 (1988) 3273–3285.
6. A. I. M. Denneman and R. J. J. Jongschaap, A bead-spring model incorporating cyclic structures, non-equal springs and beads with non-equal friction coefficients. *J. Rheol.* 40 (1996) 589–612.
7. A. I. M. Denneman, R. J. J. Jongschaap, and J. Mellema, Rheological modeling with Hookean bead-spring cubes (SC, BCC and FCC). *J. Eng. Math.* 34 (1998) 75–95.
8. A. I. M. Denneman, R. J. J. Jongschaap, and J. Mellema, Singular behavior of Rouse-like spectra. *J. Rheol.* 43 (1999) 327–337.
9. L. van Hove, The occurrence of singularities in the elastic frequency distribution of a crystal. *Phys. Rev.* 89 (1953) 1189–1193.
10. A. A. Maradudin, E. W. Montroll, G. H. Weiss, and I. P. Ipatova, *Theory of Lattice Dynamics in the Harmonic Approximation*. New York: Academic Press (2nd ed., 1971) 708 pp.
11. G. K. Fraenkel, Visco-elastic effect in solution of simple particles. *J. Chem. Phys.* 20 (1952) 642–647.
12. R. A. Horn and C. R. Johnson, *Topics in Matrix Analysis*. Cambridge: Cambridge University Press (1991) 607 pp.
13. P. J. Davis, *Circulant Matrices*. New York: John Wiley & Sons (1979) 250 pp.
14. H. Kramers, Het gedrag van macromoleculen in een stromende vloeistof. *Physica* 11 (1944) 1–19.
15. B. van der Vorst, E. M. Toose, D. van den Ende, R. J. J. Jongschaap, and J. Mellema, Generalized Rouse model for a dilute solution of clustered polymers. *Rheol. Acta* 34 (1995) 274–280.
16. M. Gottlieb and R. B. Bird, A molecular dynamics calculation to confirm the incorrectness of the random-walk distribution for describing the Kramers freely jointed bead-rod chain. *J. Chem. Phys.* 65 (1976) 2467–2468.
17. N. G. van Kampen, Statistical mechanics of trimers. *Appl. Sci. Res.* 37 (1981) 67–75.
18. A. I. M. Denneman, R. J. J. Jongschaap, and J. Mellema, A colloidal crystal modeled by bead-spring cubes. *J. Chem. Phys.* 111 (1999) 8182–8195.